Geology

Localized shear in the deep lithosphere beneath the San Andreas fault system

Heather A. Ford, Karen M. Fischer and Vedran Lekic

Geology published online 25 February 2014;
doi: 10.1130/G35128.1

Email alerting services click www.gsapubs.org/cgi/alerts to receive free e-mail alerts when new articles cite this article

Subscribe click www.gsapubs.org/subscriptions/ to subscribe to Geology

Permission request click http://www.geosociety.org/pubs/copyrt.htm#gsa to contact GSA

Copyright not claimed on content prepared wholly by U.S. government employees within scope of their employment. Individual scientists are hereby granted permission, without fees or further requests to GSA, to use a single figure, a single table, and/or a brief paragraph of text in subsequent works and to make unlimited copies of items in GSA's journals for noncommercial use in classrooms to further education and science. This file may not be posted to any Web site, but authors may post the abstracts only of their articles on their own or their organization's Web site providing the posting includes a reference to the article's full citation. GSA provides this and other forums for the presentation of diverse opinions and positions by scientists worldwide, regardless of their race, citizenship, gender, religion, or political viewpoint. Opinions presented in this publication do not reflect official positions of the Society.

Notes

Advance online articles have been peer reviewed and accepted for publication but have not yet appeared in the paper journal (edited, typeset versions may be posted when available prior to final publication). Advance online articles are citable and establish publication priority; they are indexed by GeoRef from initial publication. Citations to Advance online articles must include the digital object identifier (DOIs) and date of initial publication.

© Geological Society of America

THE GEOLOGICAL SOCIETY OF AMERICA

Geology, published online on 25 February 2014 as doi:10.1130/G35128.1

Localized shear in the deep lithosphere beneath the San Andreas fault system

Heather A. Ford[1,*], Karen M. Fischer[1], and Vedran Lekic[2]
[1]Department of Geological Sciences, Brown University, 324 Brook Street, Box 1846, Providence, Rhode Island 02912, USA
[2]Department of Geology, University of Maryland, College Park, Maryland 20742, USA

ABSTRACT

Seismic images of the base of the lithosphere across the San Andreas fault system (California, USA) yield new constraints on the distribution of deformation in the deep lithosphere beneath this strike-slip plate boundary. We show that conversions of shear to compressional waves (Sp) across the base of the lithosphere are systematically weaker on the western side of the plate boundary, indicating that the drop in seismic shear-wave velocity from lithosphere to asthenosphere is either smaller or occurs over a larger depth range. In central and northern California, the lithosphere-asthenosphere boundary changes character across a distance of <50 km, and does so directly beneath the San Andreas fault along its simple central segment, and beneath the Calaveras–Green Valley–Bartlett Springs faults to the north. Given the absolute velocities of the North America and Pacific plates, and low viscosities inferred for the asthenosphere, these results indicate the juxtaposition of mantle lithospheres with different properties across these faults. The spatial correlation between the central San Andreas fault and the laterally abrupt change in the velocity structure of the deepest mantle lithosphere points to the accommodation of relative plate motion on a narrow shear zone (<50 km in width), and a rheology that enables strain localization throughout the thickness of the lithosphere.

INTRODUCTION

The distribution of deformation in the deep mantle lithosphere beneath strike-slip plate boundaries is a widely debated, yet unresolved, aspect of plate tectonics. Models range from localized shear zones extending beneath individual crustal faults to broad zones of diffuse shear hundreds of kilometers wide, and these scenarios have different implications for the rheology of the mantle lithosphere (e.g., Bürgmann and Dresen, 2008; Bonnin et al., 2010; Platt and Behr, 2011; Titus et al., 2007; Vauchez et al., 2012; Bercovici and Ricard, 2012).

The San Andreas fault (SAF) system (California, USA) accommodates ~75% of the relative motion between the North America and Pacific plates, primarily by 23–37 mm/yr slip on the SAF (Molnar and Dayem, 2010; Rolandone et al., 2008), but also by slip on adjacent strike-slip faults (Fig. 1). In central California, strike-slip motion is almost entirely confined to the SAF, while in northern California slip is distributed in a 100 km zone of subparallel faults, including the Calaveras–Green Valley–Bartlett Springs faults in the east (Fig. 1). In southern California, the plate boundary splays into a series of parallel faults.

In contrast with its expression at and near the surface, the distribution of shear across the plate boundary at upper mantle depths has lacked clarity. Deformed xenoliths beneath the Calaveras fault (Titus et al., 2007) and steps in the crust-mantle boundary (Moho) depth across the SAF (Henstock et al., 1997; Zhu, 2000) are consistent with shear due to plate motion at the top of the mantle lithosphere. Deeper, shear-wave splitting in SKS phases in central California has been used to argue for 40-km-wide mantle shear zones beneath individual strike-slip faults and an ~130 km total shear zone width (Bonnin et al., 2010), while in southern California, SKS splitting tomography suggests a more complex pattern of deformation (Monteiller and Chevrot, 2011). Converted seismic waves, however, provide excellent resolution of the lithosphere-asthenosphere boundary (LAB), and thus offer a different means of constraining deformation in the deep mantle lithosphere. Prior converted phase studies (Abt et al., 2010; Kumar et al., 2012; Lekic et al., 2011; Levander and Miller, 2012; Li et al., 2007) have estimated lithospheric thicknesses in California, but did not note systematic changes in LAB properties across the SAF system.

*Current address: Department of Geology and Geophysics, Yale University, PO Box 208109, New Haven, Connecticut 06520-8109, USA; E-mail: heather.ford@yale.edu.

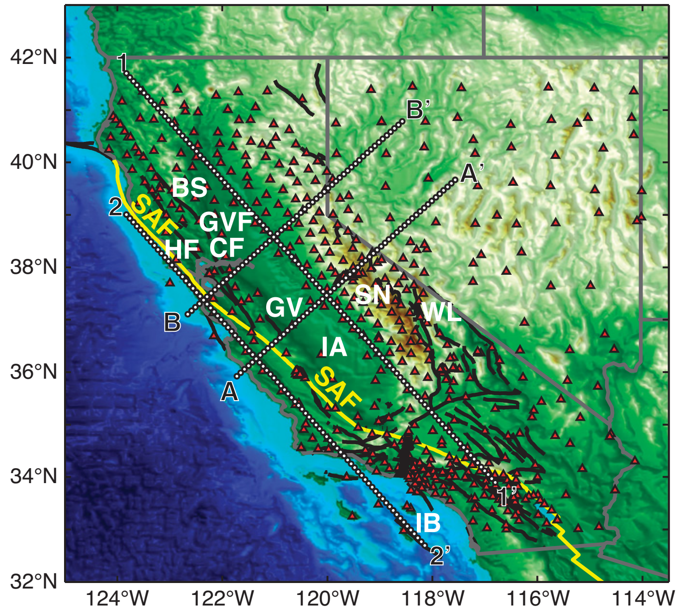

Figure 1. Map of study region. Red triangles are locations of seismic stations used in study. White dotted lines delineate cross sections shown in Figure 2. Thin black lines are faults; thick yellow line is the San Andreas fault (SAF); solid gray lines are state boundaries. Abbreviations: BS—Bartlett Springs fault, HF—Hayward fault, CF—Calaveras fault, GV—Great Valley, GVF—Green Valley fault, SN—Sierra Nevada, IA—Isabella anomaly, WL—Walker Lane, IB—inner California Borderland.

DATA AND METHODS

We calculated more than 135,000 Sp receiver functions from 730 seismic stations (Fig. 1), and stacked them according to their three-dimensional conversion point locations using a model for crust (Lowry and Pérez-Gussinyé, 2011) and mantle (Obrebski et al., 2011) velocity structure beneath each station and a spline-function representation of the Sp Fresnel zone (Lekic et al., 2011). Sp conversion points at lithosphere-asthenosphere boundary depths are very dense on both sides of the SAF, and we interpreted the Sp common conversion point (CCP) stack only at those nodes with information from more than 300 receiver functions. (See the GSA Data Repository[1] for more on methods.) Uncertainties in LAB

[1]GSA Data Repository item 2014111, additional profile examples, receiver function and stacking methods, LAB phase selection, influence of ray parameter on amplitude, and modeling LAB velocity gradient, is available online at www.geosociety.org/pubs/ft2014.htm, or on request from editing@geosociety.org or Documents Secretary, GSA, P.O. Box 9140, Boulder, CO 80301, USA.

Data Repository item 2014111 | doi:10.1130/G35128.1
© 2014 Geological Society of America. For permission to copy, contact Copyright Permissions, GSA, or editing@geosociety.org.

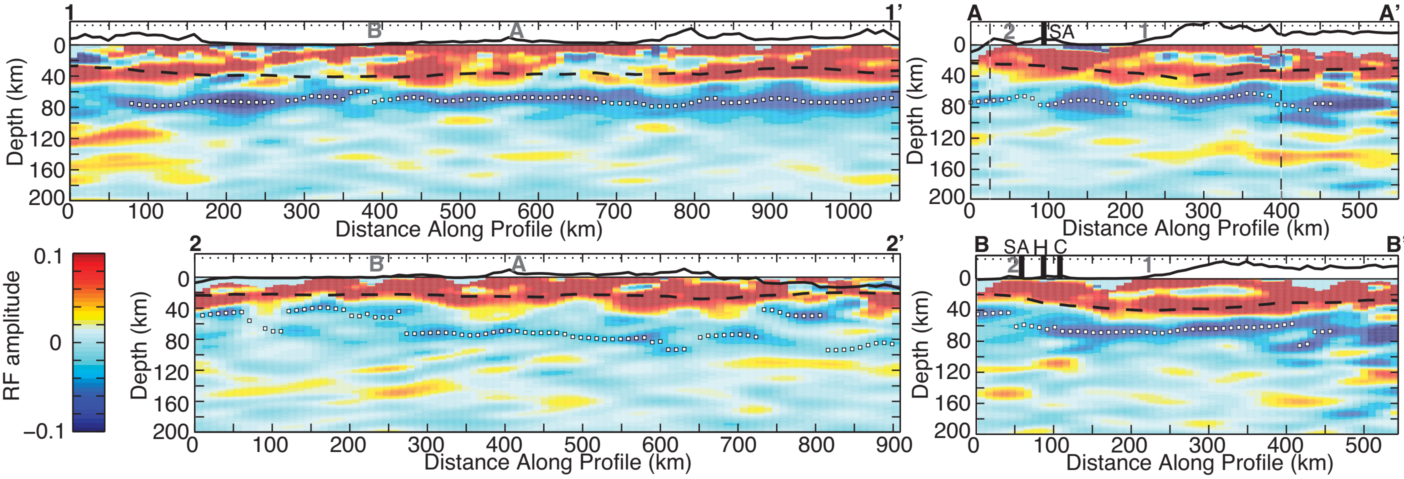

Figure 2. Vertical cross sections through Sp common conversion point stack (see text). Negative phases (blue) indicate velocity decrease with depth. White squares show depths inferred for lithosphere-asthenosphere boundary (LAB) phase (see the Data Repository [see footnote 1]). Positive amplitude phase (red) at depths of 20–40 km is interpreted to be the Moho, although conversions from intracrustal discontinuities, such as bases of sedimentary basins, also occur. Dashed black line corresponds to Ps estimates of Moho depth (Lowry and Pérez-Gussinyé, 2011). Gray labels indicate cross-section intersections; thick black lines are major faults. Surface topography is exaggerated 10×. Amplitude of inferred LAB phase is significantly weaker in 2–2′ than in 1–1′, and to west of San Andreas (SA—A–A′) and Calaveras (C—B–B′) faults. Outside of black dashed lines in A-A′ (which correspond to white dashed line in Fig. 3) LAB phase picks are less robust. Gray labels 1, 2, A, and B in cross sections correspond to intersections with other cross sections. RF—receiver function.

depth due to waveform scatter and uncertainties in the migration model are typically <±10 km.

RESULTS

Sp conversions due to a velocity decrease with depth are observed throughout the study region; the mid-point of this negative velocity gradient is at depths of 45–100 km, with an average depth of 70 km (Figs. 2 and 3). Because the velocity decrease required to produce observed Sp amplitudes (see the Data Repository) accounts for most of the shear wave speed (Vs) drop from the lithosphere to the asthenosphere inferred by surface wave tomography (Obrebski et al., 2011; Rau and Forsyth, 2011), and because its depth is consistent with tomography, we interpret the Sp phase as a conversion across the seismologically defined LAB.

Our CCP Sp model reveals a pronounced change in LAB phase amplitude across the plate boundary (Figs. 2 and 3A). East of the SAF system (e.g., cross-section 1–1′ in Fig. 2) the LAB phase is strong and spatially coherent, while to the west of the SAF (2–2′ in Fig. 2) the LAB phase is very low amplitude or absent. In central California, the change in LAB phase amplitude occurs beneath the SAF (A-A′ in Fig. 2; Fig. 3A), and in northern California the change occurs farther east (e.g., at the Calaveras fault, B-B′ in Fig. 2). The change in LAB properties beneath these faults occurs over short horizontal distances, typically 50 km or less (Figs. 2 and 3; Fig. DR1 in the Data Repository). At the periods used in this study and for depths of ~70 km, CCP-stacked Sp phases can distinguish lateral variations in discontinuity structure that occur over 50 km from those over larger distances, but they cannot resolve lateral variations of <50 km (Lekic et al., 2011). In southern California, LAB phases are typically weaker on the western side of the SAF, although there are exceptions (e.g., the inner California Borderland), and a laterally abrupt change in amplitude directly beneath the SAF is less consistently observed (Fig. 3A). The observed patterns in LAB phase amplitude cannot be explained by spatial variations in Sp path density or ray parameter (see the Data Repository).

Systematic variations in LAB depth across the SAF system are only observed in certain areas. Along much of the central segment of the SAF, LAB Sp phase depths on the western side of the SAF are within the uncertainties (±10 km) of those on the east, with the caveat that lithospheric thickness is unknown where phase amplitudes drop to nearly zero immediately to the west of the fault (A-A′ in Fig. 2). West and north of San Francisco Bay, a negative phase at 45–55 km depth hints at a zone of thinner lithosphere to the west of the SAF (B-B′ in Fig. 2; Fig. 3B). The absence of a clear LAB phase between the SAF and Calaveras fault obscures the exact position of the change in lithospheric thickness, but in profile B-B′ the thinning would need to occur over a horizontal distance of 75 km or less. Local reductions in LAB phase depth are also observed in the vicinity of the Walker Lane fault system to the east of the Sierras, the Isabella anomaly (e.g., Zandt et al., 2004) in the Great Valley, and in the inner California Borderland (e.g., Lekic et al., 2011) (Figs. 1 and 3; Fig. DR1).

To assess vertical gradients in absolute shear velocity (V_s) at the LAB, we modeled the ratio of LAB phase amplitudes for two regions located on adjacent sides of the SAF in central California, the Salinas (SALI) block to the west and the Great Valley thrust belt (GVTB) block to the east (Fig. 3A; see the Data Repository). If the decrease in V_s from lithosphere to asthenosphere occurs instantaneously in depth beneath both sides of the SAF, a 1% drop at the base of the SALI lithosphere would imply a 3.7% drop at the GVTB LAB. For a LAB V_s gradient >30 km in depth on both sides, a 1% drop beneath the SALI block would indicate a 7.9% drop beneath the GVTB block. Alternatively, the LAB V_s gradient beneath SALI could occur over a much larger depth range than the gradient beneath GVTB. This modeling confirms that LAB velocity gradients differ significantly between the east and west sides of the central SAF.

FAULT-CORRELATED CHANGES IN THE MANTLE LITHOSPHERE

The laterally abrupt changes in LAB velocity gradients indicate a contrast in the properties of the mantle lithosphere across the central segment of the SAF and the Calaveras–Green Valley–Bartlett Springs faults in the north. Sharp lateral changes correlated with these faults would be difficult to maintain in the low-viscosity asthenosphere (Freed et al., 2012), in particular because the absolute motion of the North American plate is nearly normal to the strikes of these faults in a variety of reference frames (Schellart et al., 2008). Assuming an asthenosphere of roughly constant V_s across the region, shear velocity in the deep mantle lithosphere on the western side of these faults would be smaller than on the eastern side.

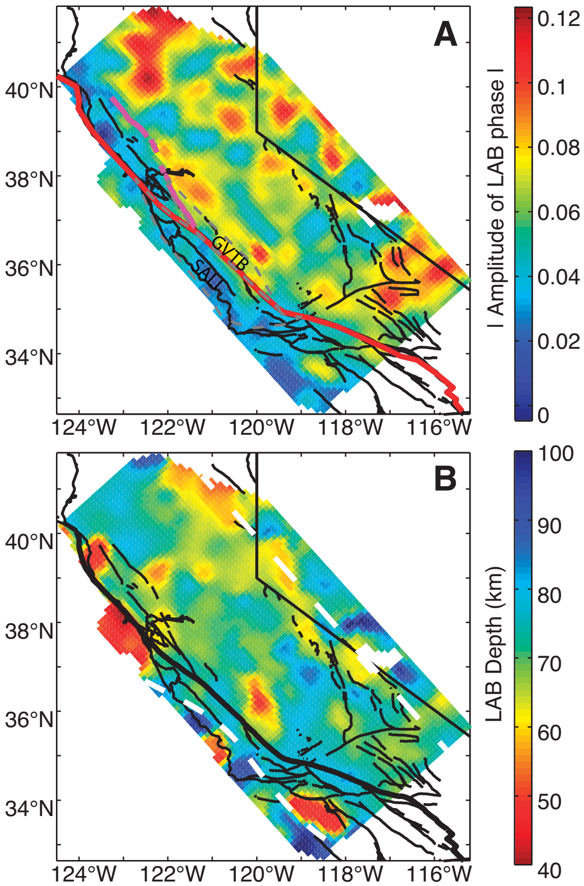

Figure 3. A: Map of lithosphere-asthenosphere boundary (LAB) phase amplitude strength. Gray dashed lines outline Salinian (SALI) and Great Valley thrust block (GVTB) crustal blocks defined by faults and plate motion (McCaffrey, 2005). San Andreas and Calaveras–Green Valley–Bartlett Springs faults are highlighted in red and magenta, respectively. Amplitudes are significantly lower west of the San Andreas and Calaveras–Green Valley–Bartlett Springs faults. Amplitude contrast is particularly sharp directly below central San Andreas. B: Map view of LAB depth. Amplitude and depth values were smoothed with Gaussian function with radius of ~33 km. White dashed lines indicate regions where LAB phase depths are less reliable, along western edge of common conversion point stack where phase amplitudes are very weak, and near its eastern edge where energy in LAB phase depth range is complex.

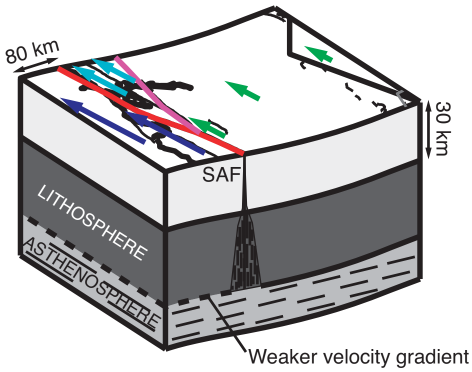

Figure 4. Schematic interpretation of lithosphere-asthenosphere boundary (LAB) Sp phase amplitude change (see text) beneath the central segment of San Andreas fault (SAF). Lithospheres with different LAB velocity gradients are juxtaposed across shear zone that is <~50 km wide at LAB. SAF and Calaveras–Green Valley–Bartlett Springs faults are highlighted in red and magenta, respectively. Vectors show plate motion with respect to North America (McCaffrey, 2005).

While this difference is seen in some regional tomographic models (Lin et al., 2010, 2012), it is not consistently present in all models (Buehler and Shearer, 2012; Obrebski et al., 2011; Rau and Forsyth, 2011), suggesting that V_s may not be reduced throughout the entire mantle lithosphere; smaller Sp amplitudes from the LAB on the Pacific side could be matched simply by a reduced V_s contrast or a more gradual V_s gradient at the base of the plate (Fig. 4), which could be undetected by tomography. Variations in V_s anisotropy at the LAB are not an obvious explanation for the fault-correlated differences in LAB phase amplitude. Azimuthal anisotropy from surface wave (Lin et al., 2010) and Pn (Buehler and Shearer, 2012) tomography and anisotropic layering inferred from shear-wave splitting in SKS phases (Bonnin et al., 2010) indicate azimuthal anisotropy with a fast direction that is approximately parallel to the direction of shearing in the lithosphere along the plate boundary and more east-west in the asthenosphere. However, none of these studies show lateral variation in azimuthal anisotropy that correlates with the observed shift in LAB phase amplitudes at the SAF in central California and the Calaveras–Green Valley–Bartlett Springs faults in northern California.

Along the central segment of the SAF, the laterally abrupt changes in properties of the deep lithosphere indicate that plate boundary shear is localized over a comparable length scale at the LAB. If the zone of shear were more broadly distributed (>100 km), maintaining the correlation between structure at the LAB and the surface trace of the fault in regions where fault strike changes substantially and as hundreds of kilometers of offset accumulated would require a large and unappealing degree of coincidence. The width of deep mantle shear across the SAF north of ~37°N is more difficult to constrain, but if the shallow (45–55 km deep) negative Sp phase at the edge of the Sp CCP stack represents thinner lithosphere to the west of the SAF (B-B′ in Fig. 2; Fig. 3B), the offset in LAB depth would suggest that shear is distributed over <~75 km. In southern California, the transition in LAB properties does not consistently occur over short (<50 km) horizontal distances directly beneath the SAF, leaving open, but not requiring, the possibility that plate boundary deformation is distributed over a wider zone at the LAB.

The horizontally localized lithospheric offsets we infer in central California are not inconsistent with the wider zone of azimuthal anisotropy in the lithosphere aligned with shear due to relative plate motion (e.g., Bonnin et al., 2010; Buehler and Shearer, 2012; Lin et al., 2010). Because seismic anisotropy can develop at relatively low strains and saturates at moderate strains (e.g., Ribe, 1992), shear-wave splitting and regional models of azimuthal anisotropy may detect weak deformation distributed over large horizontal length scales, whereas the localized variation in LAB properties we observe across the central SAF could reflect a zone of focused shear that accommodates most of the relative plate motion.

One possible origin for the contrast in lithospheric properties across the central SAF is that the deep lithosphere to the west of the fault is made up of oceanic plate underthrust eastward beneath the continental margin prior to the onset of right-lateral strike-slip motion between the Pacific and North America plates ca. 30 Ma (Brocher et al., 1999; Henstock et al., 1997). While the high-velocity layer taken as evidence for underthrust oceanic crust terminates at the SAF along its central segment, the oceanic plate has been inferred to extend farther to the east north of lat ~37°N, providing an explanation for why the contrast in LAB Sp phase amplitude shifts to the Calaveras–Green Valley–Bartlett Springs faults (Brocher et al., 1999; Henstock et al., 1997). The oceanic lithosphere would have been young when accreted, and its LAB velocity gradient could be distinct due to differences in thermal history, chemical depletion, volatile content, grain size, and melt infiltration (e.g., Fischer et al., 2010) relative to the continental lithosphere to the east of the SAF.

CONCLUSIONS

Sp receiver function stacks reveal a westward decrease in the vertical velocity gradient at the LAB across the SAF system. In central California, the change in the LAB velocity gradient occurs beneath the SAF over a horizontal distance of <50 km, whereas in northern California, a comparably sharp lateral change in LAB properties occurs beneath the Calaveras–Green Valley–Bartlett Springs faults. These results indicate that mantle lithospheres with different basal properties are juxtaposed across these faults. Beneath the central segment of the SAF, deformation appears to extend through the lithosphere in a relatively narrow shear zone (<~50 km in width). This result supports the view that the mantle lithosphere, as defined by seismic velocities, is relatively plate like and deforms only in focused zones of deformation, consistent with rheological models that allow localized strain throughout the mantle lithosphere (e.g., Bercovici and Ricard, 2012).

ACKNOWLEDGMENTS

We thank Don Forsyth, Greg Hirth, and Marc Parmentier for discussions, and Rob McCaffrey for the block models used in this paper. Waveforms were obtained from the IRIS (Incorporated Research Institutions for Seismology) Data Management Center and the Northern and Southern California Earthquake Data Centers. This work was supported by the National Science Foundation EarthScope Program (grant EAR-0641772).

REFERENCES CITED

Abt, D.L., Fischer, K.M., French, S.W., Ford, H.A., Yuan, H., and Romanowicz, B., 2010, North American lithospheric discontinuity structure imaged by Ps and Sp receiver functions: Journal of Geophysical Research, v. 115, B09301, doi:10.1029/2009JB006914.

Bercovici, D., and Ricard, Y., 2012, Mechanisms for the generation of plate tectonics by two-phase grain damage and pinning: Physics of the Earth and Planetary Interiors, v. 202–203, p. 27–55, doi:10.1016/j.pepi.2012.05.003.

Bonnin, M., Barruol, G., and Bokelmann, G.H., 2010, Upper mantle deformation beneath the North American–Pacific plate boundary in California from SKS splitting: Journal of Geophysical Research, v. 115, B04306, doi:10.1029/2009JB006438.

Brocher, T.M., Brink, U.S., and Abramovitz, T., 1999, Synthesis of crustal seismic structure and implications for the concept of a slab gap beneath coastal California: International Geology Review, v. 41, p. 263–274, doi:10.1080/00206819909465142.

Buehler, J.S., and Shearer, P.M., 2012, Localized imaging of the uppermost mantle with USArray Pn data: Journal of Geophysical Research, v. 117, B09305, doi:10.1029/2012JB009433.

Bürgmann, R., and Dresen, G., 2008, Rheology of the lower crust and upper mantle: Evidence from rock mechanics, geodesy, and field observations: Annual Review of Earth and Planetary Sciences, v. 36, p. 531–567, doi:10.1146/annurev.earth.36.031207.124326.

Fischer, K.M., Ford, H.A., Abt, D.L., and Rychert, C.A., 2010, The lithosphere-asthenosphere boundary: Annual Review of Earth and Planetary Sciences, v. 38, p. 551–575, doi:10.1146/annurev-earth-040809-152438.

Freed, A.M., Hirth, G., and Behn, M.D., 2012, Using short-term postseismic displacements to infer the ambient deformation conditions of the upper mantle: Journal of Geophysical Research, v. 117, B01409, doi:0.1029/2011JB008562.

Henstock, T.J., Levander, A., and Hole, J.A., 1997, Deformation in the lower crust of the San Andreas fault system in northern California: Science, v. 278, p. 650–653, doi:10.1126/science.278.5338.650.

Kumar, P., Kind, R., Yuan, X., and Mechie, J., 2012, USArray receiver function images of the lithosphere-asthenosphere boundary: Seismological Research Letters, v. 83, p. 486–491, doi:10.1785/gssrl.83.3.486.

Lekic, V., French, S.W., and Fischer, K.M., 2011, Lithospheric thinning beneath rifted regions of southern California: Science, v. 334, p. 783–787, doi:10.1126/science.1208898.

Levander, A., and Miller, M.S., 2012, Evolutionary aspects of lithosphere discontinuity structure in the western US: Geochemistry Geophysics Geosystems, v. 13, Q0AK07, doi:10.1029/2012GC004056.

Li, X., Yuan, X., and Kind, R., 2007, The lithosphere-asthenosphere boundary beneath the western United States: Geophysical Journal International, v. 170, p. 700–710, doi:10.1111/j.1365-246X.2007.03428.x.

Lin, F.C., Ritzwoller, M.H., Yang, Y., Moschetti, M.P., and Fouch, M.J., 2010, Complex and variable crustal and uppermost mantle seismic anisotropy in the western United States: Nature Geoscience, v. 4, p. 55–61, doi:10.1038/ngeo1036.

Lin, F.C., Schmandt, B., and Tsai, V.C., 2012, Joint inversion of Rayleigh wave phase velocity and ellipticity using USArray: Constraining velocity and density structure in the upper crust: Geophysical Research Letters, v. 39, L12303, doi:10.1029/2012GL052196.

Lowry, A.R., and Pérez-Gussinyé, M., 2011, The role of crustal quartz in controlling Cordilleran deformation: Nature, v. 471, p. 353–357, doi:10.1038/nature09912.

McCaffrey, R., 2005, Block kinematics of the Pacific–North America plate boundary in the southwestern United States from inversion of GPS, seismological, and geologic data: Journal of Geophysical Research, v. 110, B07401, doi:10.1029/2004JB003307.

Molnar, P., and Dayem, K.E., 2010, Major intracontinental strike-slip faults and contrasts in lithospheric strength: Geosphere, v. 6, p. 444–467, doi:10.1130/GES00519.1.

Monteiller, V., and Chevrot, S., 2011, High-resolution imaging of the deep anisotropic structure of the San Andreas fault system beneath southern California: Geophysical Journal International, v. 186, p. 418–446, doi:10.1111/j.1365-246X.2011.05082.x.

Obrebski, M., Allen, R.M., Pollitz, F., and Hung, S.H., 2011, Lithosphere-asthenosphere interaction beneath the western United States from the joint inversion of body-wave traveltimes and surface-wave phase velocities: Geophysical Journal International, v. 185, p. 1003–1021, doi:10.1111/j.1365-246X.2011.04990.x.

Platt, J.P., and Behr, W.M., 2011, Lithospheric shear zones as constant stress experiments: Geology, v. 39, p. 127–130, doi:10.1130/G31561.1.

Rau, C.J., and Forsyth, D.W., 2011, Melt in the mantle beneath the amagmatic zone, southern Nevada: Geology, v. 39, p. 975–978, doi:10.1130/G32179.1.

Ribe, N.M., 1992, On the relation between seismic anisotropy and finite strain: Journal of Geophysical Research, v. 97, p. 8737–8747, doi:10.1029/92JB00551.

Rolandone, F., Bürgmann, R., Agnew, D.C., Johanson, I.A., Templeton, D.C., d'Alessio, M.A., Titus, S.J., DeMets, C., and Tikoff, B., 2008, Aseismic slip and fault-normal strain along the central creeping section of the San Andreas fault: Geophysical Research Letters, v. 35, L14305, doi:10.1029/2008GL034437.

Schellart, W.P., Stegman, D.R., and Freeman, J., 2008, Global trench migration velocities and slab migration induced upper mantle volume fluxes: Constraints to find an Earth reference frame based on minimizing viscous dissipation: Earth and Planetary Science Letters, v. 88, p. 118–144.

Titus, S.J., Medaris, L.G., Wang, H.F., and Tikoff, B., 2007, Continuation of the San Andreas fault system into the upper mantle: Evidence from spinel peridotite xenoliths in the Coyote Lake basalt, central California: Tectonophysics, v. 429, p. 1–20, doi:10.1016/j.tecto.2006.07.004.

Vauchez, A., Tommasi, A., and Mainprice, D., 2012, Faults (shear zones) in the Earth's mantle: Tectonophysics, v. 558–559, p. 1–27, doi:10.1016/j.tecto.2012.06.006.

Zandt, G., Gilbert, H., Owen, T.J., Ducea, M., Saleeby, J., and Jones, C., 2004, Active foundering of a continental arc root beneath the southern Sierra Nevada in California: Nature, v. 431, p. 41–46, doi:10.1038/nature02847.

Zhu, L., 2000, Crustal structure across the San Andreas fault, southern California from teleseismic converted waves: Earth and Planetary Science Letters, v. 179, p. 183–190, doi:10.1016/S0012-821X(00)00101-1.

Manuscript received 19 September 2013
Revised manuscript received 31 December 2013
Manuscript accepted 10 January 2014

Printed in USA